

Copy-Move Detection in Optical Microscopy: A Segmentation Network and A Dataset

Hao-Chiang Shao[†], *Member, IEEE*, Yuan-Rong Liao, Tse-Yu Tseng, Yen-Liang Chuo, and Fong-Yi Lin

Abstract—With increasing revelations of academic fraud, detecting forged experimental images in the biomedical field has become a public concern. The challenge lies in the fact that copy-move targets can include background tissue, small foreground objects, or both, which may be out of the training domain and subject to unseen attacks, rendering standard object-detection-based approaches less effective. To address this, we reformulate the problem of detecting biomedical copy-move forgery regions as an intra-image co-saliency detection task and propose CMSeg-Net, a copy-move forgery segmentation network capable of identifying unseen duplicated areas. Built on a multi-resolution encoder-decoder architecture, CMSeg-Net incorporates self-correlation and correlation-assisted spatial-attention modules to detect intra-image regional similarities within feature tensors at each observation scale. This design helps distinguish even small copy-move targets in complex microscopic images from other similar objects. Furthermore, we created a copy-move forgery dataset of optical microscopic images, named FakeParaEgg, using open data from the ICIP 2022 Challenge to support CMSeg-Net’s development and verify its performance. **Extensive experiments demonstrate that our approach outperforms previous state-of-the-art methods on the FakeParaEgg dataset and other open copy-move detection datasets, including CASIA-CMFD, CoMoFoD, and CMF. The FakeParaEgg dataset, our source code, and the CMF dataset with our manually defined segmentation ground truths are available at <https://github.com/YoursEver/FakeParaEgg>.**

Index Terms—Copy-move forgery detection, Attention, Multiresolution, Optical microscopy images, co-saliency.

I. INTRODUCTION

Biomedical image forgery issues have garnered public attention due to recent, ongoing revelations of academic fraud or misconduct [1], [2], [3], [4]. Accusations of falsification emerging on platforms such as the “PubPeer” forum cast doubt even on esteemed scholars and previously influential research works. These cases typically involve illegal instances of image reuse or manipulation, often employing illicit post-processing approaches like deliberate cropping and copy-move manipulations [5]. Identifying such falsifications poses a significant challenge for publishers and researchers, and thus there is a growing public concern for methods capable of detecting fraudulent biomedical images.

In real-world academic fraud cases, two common types of biomedical image manipulation are **copy-move** and **image reuse** [6], the latter of which can be considered a form of

copy-move forgery when the reused region appears alongside its source image. However, typical copy-move detection methods, often developed using an object detection backbone and natural image datasets, may struggle to identify duplications in biomedical images. This is because biomedical images frequently contain foreground objects with similar geometric shapes and uniform appearances, while their backgrounds often feature patterns resembling the foreground. Additionally, biomedical images involve texture patterns that are not adequately addressed by natural image datasets. As a result, few forgery detectors are specialized for the biomedical domain.

To address these challenges, we created a microscopic copy-move image dataset named **FakeParaEgg** using the public data provided by the *ICIP 2022 Challenge: Parasitic Egg Detection and Classification in Microscopic Images* [7], [8]. Additionally, we redefined the copy-move detection task as an intra-image co-saliency detection problem, targeting duplicated regions within an image—whether foreground objects or background tissues. Accordingly, we devised a copy-move segmentation network (CMSeg-Net) capable of segmenting co-salient regions with out-of-domain unseen patterns by exploiting intra-image regional similarities in a multiresolution fashion.

This paper thus makes three contributions. First, we reframe the copy-move forgery detection problem as an intra-image co-saliency detection issue and propose a lightweight segmentation model that is robust against **out-of-domain patterns even when exposed to unseen attacks such as background removal, compression, and scaling, which are commonly encountered in academic fraud investigations**. Second, we introduce a correlation-assisted spatial-attention (CoSA) module to enhance the recognition of multiple intra-image duplicated regions, including small foreground objects and those similar to background areas, within the images. Third, we introduce **and release** an optical microscopic copy-move forgery image dataset, named **FakeParaEgg**, with this paper to facilitate the future advancement of academic fraud detection techniques.

II. RELATED WORKS

Recent copy-move detection methods can be categorized into two groups: those relying on modern convolutional neural networks (CNN) and those employing conventional strategies such as feature-based methods and manual inspections for real-world academic misconduct investigations. Modern CNN-based approaches, typically address the copy-move detection problem by treating it as an object detection task. For example, Dense-InceptionNet [9] utilizes a single-branch dense-net

Manuscript received on June 12, 2024. This work was supported in part by NSTC 112-2221-E-005-080 and iGroup Asia-Pacific. (Corresponding Author: Prof. H.-C. Shao; Email: shao.haochiang@gmail.com)

H.-C. Shao, Y.-L. Chuo, and F.-Y. Lin are with the Institute of Data Science and Information Computing, National Chung Hsing University, Taiwan.

Y.-R. Liao is with SOE Technology Inc., Taiwan.

T.-Y. Tseng is with iGroup (Asia-Pacific) Ltd., Taiwan.

based pyramid feature extractor to facilitate feature correlation matching for copy-move detection, while RGB-N [10] and BusterNet [11] employ a two-branch architecture for detecting similar objects based on matched features. In addition, some literature, such as Mantra-Net [12], views copy-move detection as a local anomaly detection issue and employs anomaly detection strategies to identify local forgeries. Another category of approaches tackles this problem using segmentation strategies centered around a feature affinity matrix, exemplified by RRU-Net [13] and DOA-GAN [14]. Recent methods of this kind, such as SelfDM-SA [15], CMFDFormer [16], and UCM-Net [17], leverage the attention mechanism—widely used in computer vision applications, such as [18], [19]—to construct a sophisticated feature extraction backbone. This backbone enables the network model to provide a segmentation result with the improved assistance of intra-image correlation computations. However, these methods were primarily designed for natural images, and experiments indicate their inadequacy in handling real-world biomedical copy-move forgeries.

In contrast, traditional feature-based methods identify copy-move regions by matching descriptors of high-level features. Examples include the dense-field approach by Cozzolino et al. [20], Pun et al.'s regional feature point matching method [21], and the hierarchical feature point matching method by Li and Zhou [22]. However, these methods face challenges when applied to images with weak edges or indistinct feature points, such as gel electrophoresis images or microscopic images containing semi-transparent foreground objects. Consequently, manual inspection remains a key tool in academic misconduct investigations, as highlighted by Piller [2]. This highlights the need for a new dataset and an improved copy-move detector.

III. METHOD

By reformulating the copy-move detection task as an intra-image co-saliency detection problem, we develop CMSeg-Net (Copy-move Segmentation Net), which aims to identify regions with highly correlated features. CMSeg-Net utilizes an encoder-decoder structure, commonly adopted in previous co-saliency detection networks [23], [24], with a MobileNet-v2 [25] encoder for feature representability and lightweight purposes. Additionally, to derive inter-pixel feature correlation for detecting duplicated copy-move regions, we design a correlation-assisted spatial-attention (CoSA) module. This module consists of a correlation submodule (CoR) and a spatial attention submodule with a variable-sized receptive field (VRSA), implemented by incorporating the spatial attention module [26] with a variable receptive field adopted in the atrous spatial pyramid pooling layer [27]. Finally, to efficiently re-organize the feature tensors enhanced by CoSA modules, we adopt the inverted residual block (IRB) to accomplish the decoding path of CMSeg-Net, reducing the memory requirement [25]. The framework is depicted in Fig. 1

In the CMSeg-Net design, a MobileNet-v2 pretrained on ImageNet [28] serves as the initial encoder for the learning process. This choice is motivated by real-world copy-move scenarios in which any object could be a potential forgery target, necessitating a feature extraction backbone capable of

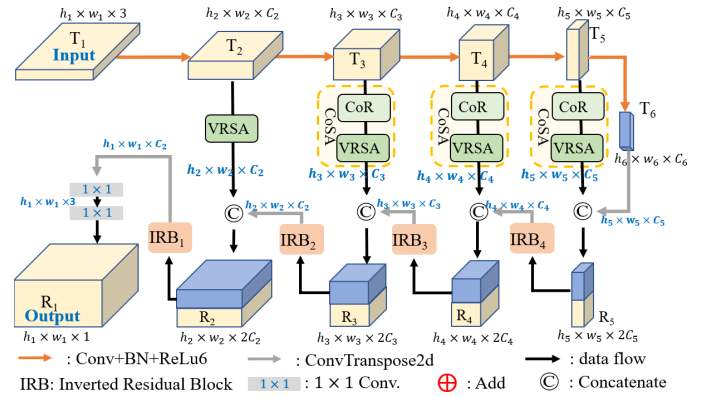


Fig. 1. Architecture of the **CMSeg-Net**. The encoding path from T_1 to T_6 follows MobileNetV2, using ReLU6 activation for robustness, while the decoding path from R_5 to R_1 utilizes the *inverted residual block* (IRB) for reconstruction. The VRSA block enhances its input with a spatial attention submodule featuring a variable-sized receptive field, while the CoR block derives spatial correlation for copy-move detection. Note that $C_2 = 16$, $C_3 = 24$, $C_4 = 32$, $C_5 = 96$, $C_6 = 1280$, and $(h_{i+1}, w_{i+1}) = (\frac{1}{2}h_i, \frac{1}{2}w_i)$.

deriving intricate features from complex scenes. Based on the feature tensors extracted by the MobileNet-v2 encoder, CMSeg-Net employs a CoSA module to evaluate intra-image feature correlations and identify highly correlated spatial positions within the mid-level feature tensors. Subsequently, the submodule refines the feature tensor based on the contribution from the i -th pixel to the j -th pixel, guaranteeing accurate detection and segmentation of copy-move areas. Note that only the feature tensors of the three intermediate levels, *i.e.*, T_3 , T_4 , and T_5 , are processed by the full CoSA module, while the CoSA module is simplified for the T_2 tensor and neglected for the T_6 tensor. This is because the deepest/topmost feature captures too global/local information, which is not effective in identifying copy-move areas. The details of our CMSeg-Net design will be elaborated in the following subsections.

- **Correlation Submodule (CoR):** The CoR module is designed to capture the intra-image similarity of a copy-move forgery image. Given a feature tensor T_i with size $h_i \times w_i \times C_i$, the CoR module first derives an $(h_i w_i) \times (h_i w_i)$ initial affinity matrix \hat{A}_i as $\hat{A}_i = F_i^T F_i$, and F_i is a $C_i \times (h_i w_i)$ reshaped version of T_i with its column vectors normalized. Clearly, $\hat{A}_i(s, t)$ records the cosine similarity between the feature vectors of the s -th and the t -th positions. Then, we obtain the affinity matrix $A_i = \hat{A}_i \odot \Phi_i$ by suppressing the self-similarity around the main diagonal of \hat{A}_i with a suppression matrix Φ_i . Here, $\Phi_i(s, t) = 1 - e^{-\frac{(s_x - t_x)^2 + (s_y - t_y)^2}{2\gamma^2}}$ with γ typically ranging between 3 and 5 by default; (s_x, s_y) and (t_x, t_y) are respectively the coordinates of s and t on the $h_i \times w_i$ domain; and, \odot denotes the Hadamard product. Because the second term of Φ_i is a radial basis function, $\Phi_i(s, t)$ approaches 0 when s 's coordinate approaches t 's, and therefore the self-similarity around the main diagonal of \hat{A}_i can be suppressed. Finally, we reshape A_i back to a $(h_i w_i) \times h_i \times w_i$ tensor, and then follow Liu et al.'s [15] strategy to output a $k \times h_i \times w_i$ tensor K by selecting the k largest values of each $(h_i w_i) \times 1 \times 1$ vector in descending order.

- **Spatial attention with variable-sized receptive field**

(VRSA): Our VRSA submodule consists of an atrous spatial pyramid pooling (ASPP) block [27] and a spatial attention (SAM) block used in CBAM [26]. In CMSEg-Net, the ASPP block is implemented with four 3×3 convolutional layers using dilation rates of $\{4, 8, 12, 16\}$ to extract contextual features from the tensor \mathbf{K} at different fields of view. The resulting four feature maps are concatenated and then fed into a 1×1 convolution layer to derive the tensor $\tilde{\mathbf{K}}_i$ that captures local and image-level features. Finally, this tensor is further fed into a spatial attention block to yield $\mathbf{B}_i = \tilde{\mathbf{K}}_i + M_s(\tilde{\mathbf{K}}_i)$. Here, $M_s(\cdot) \in \mathbb{R}^{H \times W}$ is the spatial attention map defined as $M_s(\tilde{\mathbf{K}}_i) = \sigma(f^7(\tilde{\mathbf{K}}_i))$, where σ and f^7 denote the sigmoid function and a 7×7 convolution layer, respectively.

•**Decoding Path:** CMSEg-Net’s decoding path structurally mirrors the multi-resolution reconstruction framework used in wavelet and pyramid analysis [29], [30]. This design leads to the reconstruction result $R_i = B_i \odot f_i^d(\text{IRB}_i(R_{i+1}))$ for $2 \leq i \leq 4$. Here, $f_i^d(\cdot)$ denotes the **ConvTranspose2D** routine for the tensor derived by the *inverted residual block* [27] at the i -th scale in the decoding path, and $B_i = \text{CoSA}(T_i)$. Note that in order to fit the hardware limitation, the CoSA module for T_2 consists of only a VRSA submodule, and the CoR submodule is omitted. Additionally, the CoSA module for T_6 is omitted because T_6 has too coarse a spatial resolution to capture inter-region spatial correlations.

•**Total Loss:** As a segmentation network, CMSEg-Net is trained using binary cross-entropy loss and Dice loss.

IV. EXPERIMENT RESULT

A. Datasets

We evaluate the model performance on the **FakeParaEgg**, **CASIA-CMFD**, **CoMoFoD** [31], and **CMF** [32] datasets.

FakeParaEgg is our self-made microscopic image dataset designed to simulate copy-move manipulations commonly encountered in real-world academic fraud cases. Unlike existing open datasets, FakeParaEgg consists of forgery images where foreground objects have had their backgrounds removed (i.e., made transparent), making these copy-moves difficult to detect using traditional methods due to the nonidentical background context. Moreover, **FakeParaEgg** introduces a wide range of complexities, including low-contrast dark backgrounds, high-contrast bright backgrounds, nearly transparent foreground objects, and both simple and complex backgrounds. It also features varied foreground sizes, making it a highly diverse resource for developing robust detection methods for academic fraud investigations. **FakeParaEgg** contains 1,400 forged images for training and 100 for testing. To create it, we cropped parasitic eggs using ground-truth bounding boxes from [7], removed the backgrounds using **Rembg** [33], and randomly pasted the background-free patches onto the original image, producing the final synthetic copy-move forgeries.

Additionally, **CASIA-CMFD**, a subset of **CASIA V2.0** [34], contains 1,309 copy-move images and is widely used for performance evaluation in copy-move detection studies. **CoMoFoD** and **CMF** are used to assess the model’s generalizability on out-of-domain (OOD) data with unseen attacks. **CoMoFoD** includes 25 categories, covering geometrical attacks (F), brightness changes (BC), contrast adjustments (CA),

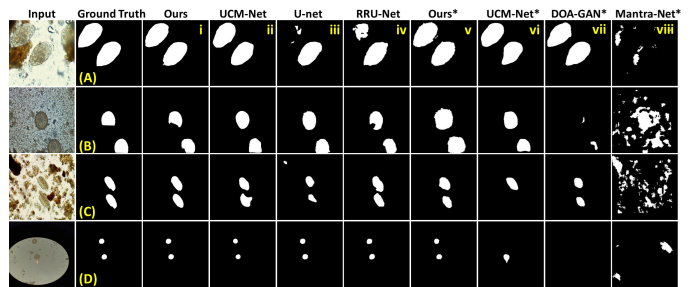


Fig. 2. Visual performance comparison among methods on **FakeParaEgg**. Note that Columns iv-vii are out-of-domain generalizability tests.

TABLE I
PERFORMANCE COMPARISON ON **FAKEPARAEgg**. (A) SINGLE DOMAIN TESTS, (B) **OUT-OF-DOMAIN GENERALIZABILITY TESTS**

	Method	mF1	mIoU	Prec.	Recall	Spec.
(A)	U-Net [35]	.749	.616	.770	.855	.9934
	RRU-Net [13]	.777	.652	.788	.898	.9938
	UCM-Net [17]	.713	.586	.782	.867	.9937
	Ours	.922	.885	.878	.970	.9972
(B)	ManTra-Net [12]	.099	.060	.094	.280	.9302
	DOA-GAN [14]	.390	.315	.792	.603	.9959
	UCM-Net [17]	.478	.396	.714	.742	.9923
	Ours	.739	.582	.828	.667	.9962

color reduction (CR), image blurring (IB), JPEG compression (JC), and noise addition (NA), with varying levels of attack intensity, each consisting of 200 attacked copy-move samples. In contrast, **CMF** has 17 categories, including no attack (Non), scaling with rotation (SR), mirroring (MIR), rotation (Ro), and scaling (Sc), each with 15 samples.

B. Result and Discussion

FakeParaEgg: Fig. 2 (Columns i-iv) demonstrates the copy-move detection results on samples from the **FakeParaEgg** dataset. These experimental results confirm that our method effectively detects and segments copy-move regions in intricate microscopic scenes. Even in scenes with small, similar objects or complex backgrounds, our method successfully identifies forged areas. Table I summarizes the performance metrics of several copy-move detection schemes on the **FakeParaEgg** dataset. Our CMSEg-Net outperforms previous approaches in terms of mean F1 and mean IoU values. Note that the U-net here serves as a performance baseline, trained using copy-move images and their corresponding ground-truth segmentation masks with binary cross-entropy loss. Additionally, Fig. 2 (Columns v-viii) and Table I(B) present a comparison of **out-of-domain generalizability**. In this experiment, our CMSEg-Net was trained on CASIA-CMFD and tested on FakeParaEgg, while the test results for the other three methods were derived from their officially released best models. This experiment demonstrates CMSEg-Net’s robustness on bio-images outside the training domain.

CASIA-CMFD: Table II and Fig. 3 present a performance comparison between our CMSEg-Net and previous state-of-the-art methods on CASIA-CMFD. This comparison further underscores the effectiveness of CMSEg-Net in general copy-move forgery detection tasks. Also, CMSEg-Net performs reliably even in scenarios of (i) **copy-move of background**

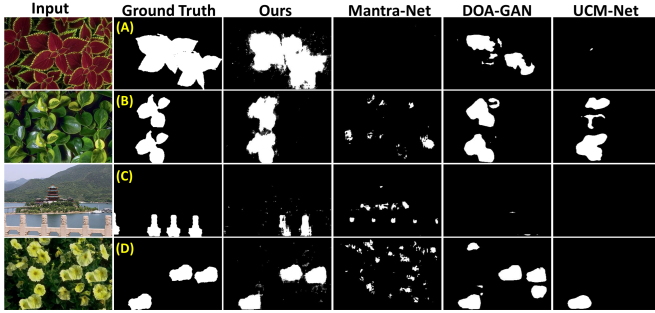


Fig. 3. Visual performance comparison of our method against ManTra-Net, DOA-GAN, and UCM-Net on the CASIA-CMFD dataset.

TABLE II
COMPARISON OF MODEL PERFORMANCE ON CASIA-CMFD

Method	mF1	Prec.	Recall	Spec.	Time(ms)	#Para.(M)
Busternet [11]	.456	.524	.692	.942	10.91	15.53
RGB-N [10]	.408	–	–	–	–	–
RRU-Net [13]	.212	.267	.255	.921	13.41	4.10
ManTra-Net [12]	.060	.450	.042	.994	46.93	3.81
DenseIncept. [9]	.643	.709	.589	–	–	–
DOA-GAN [14]	.462	.790	.505	.985	8.60	26.97
AR-Net [36]	.455	.583	.373	–	–	–
SD-Net [37]	.481	.575	.513	–	–	–
UCM-Net [17]	.543	.792	.627	.982	23.37	11.14
Ours	.643	.887	.505	.992	12.13	5.16

TABLE III
GENERALIZABILITY TESTS ON OOD DATA WITH UNSEEN ATTACKS. THE NUMBERS INDICATE THE COUNTS OF DETECTED MASKS WITH F1 > 0.5.

(A) CoMoFoD [31]						
Attack	BusterNet 2018 [11]	RRU-Net 2019 [13]	ManTra-Net 2019 [12]	DOA-GAN 2020 [14]	UCM-Net 2024 [17]	Ours
F	117	25	13	102	89	112
BC1	116	25	10	104	88	110
BC2	115	23	9	104	90	110
BC3	109	24	9	100	93	109
CA1	117	25	10	103	89	116
CA2	116	27	11	103	92	117
CA3	116	26	14	103	94	117
CR1	117	25	13	103	89	113
CR2	116	25	13	103	88	114
CR3	116	23	12	102	88	114
IB1	113	27	6	93	91	112
IB2	98	25	3	80	102	123
IB3	93	20	3	72	84	117
JC1	60	25	7	77	85	94
JC2	77	29	14	82	87	107
JC3	86	26	8	91	87	111
JC4	103	26	9	94	84	117
JC5	99	25	11	95	89	118
JC6	101	25	12	94	87	115
JC7	107	22	7	97	87	116
JC8	109	23	10	100	91	116
JC9	106	28	10	97	85	114
NA1	100	26	3	56	82	67
NA2	102	24	8	62	77	86
NA3	–	21	21	95	87	118
Total	2509	620	246	2312	2205	2763
(B) CMF [32]						
Attack	BusterNet	RRU-Net	ManTra-Net	DOA-GAN	UCM-Net	Ours
Non	14	5	2	14	15	14
SR1	13	6	2	14	14	15
SR2	13	4	3	14	15	15
SR3	10	6	1	11	13	14
SR4	1	5	1	1	8	7
SR5	2	5	2	1	6	8
MIR	3	3	2	1	11	15
Ro1	13	5	1	14	15	15
Ro2	3	6	1	4	9	9
Ro3	2	5	2	0	2	4
Ro4	0	4	2	0	1	2
Ro5	0	5	1	0	0	2
Sc1	10	3	0	10	12	14
Sc2	13	5	0	14	15	15
Sc3	14	4	3	14	15	15
Sc4	13	4	4	14	15	14
Sc5	12	5	4	11	14	12
Total	136	80	31	137	180	190

textures (see Fig. 3(A) and (B)), and (ii) multiple copy-move objects (see Fig. 3(C) and (D)).

TABLE IV
ABLATION STUDY ON CASIA-CMFD DATASET

CoR	VRSA		IRB	mF1	mIoU	Prec.	Recall	Spec.
	ASPP	SAM						
–	–	–	–	.174	.020	.555	.181	.980
–	v	v	v	.261	.147	.506	.176	.979
v	–	–	v	.169	.127	.496	.180	.979
v	v	–	v	.598	.407	.904	.447	.994
v	–	v	v	.268	.129	.515	.181	.979
v	v	v	–	.475	.286	.877	.326	.994
v	v	v	v	.643	.437	.887	.505	.992

CoMoFoD & CMF: Table III demonstrates CMSeg-Net’s generalizability against out-of-domain (OOD) copy-move images with unseen attacks. All models were trained on CASIA-CMFD, and an attacked copy-move image was considered successfully detected if its detected mask achieved $F1 > 0.5$. This experiment evidences that CMSeg-Net is the most robust against OOD data with attacks such as brightness changes (BC), contrast adjustments (CA), JPEG compression (JC), scaling with rotation (SR), and mirroring (MIR), which are commonly used in real-world image forgery cases.

Moreover, because CMSeg-Net detects areas of high co-saliency within an image as potential copy-move regions, discrepancies may arise between the detected areas and the groundtruth masks when co-saliency is insufficiently strong due to features from neighboring regions, as demonstrated in Fig. 2 and Fig. 3. Additionally, CMSeg-Net’s high precision and high specificity, as shown in Tables I and II, highlight its ability to reduce false positives while maintaining accuracy, even in complex scenarios. Notably, Table II also includes the computational time and parameter counts for several models. With a smaller parameter count and superior performance, CMSeg-Net proves to be an efficient and effective solution for copy-move forgery detection.

C. Ablation Study

Table IV presents the ablation study. The baseline model in the first row is a vanilla encoder-decoder network with a pretrained MobileNet-v2 encoder. The results indicate that the VRSA module (consisting of ASPP and SAM) contributes the most to the model’s performance. Other components, such as the CoR module with Φ_i and the IRB blocks in the decoding path, are also critical to the CMSeg-Net design.

V. CONCLUDING REMARKS

In this paper, we introduced CMSeg-Net for identifying within-image copy-move regions based on intra-image co-saliency. CMSeg-Net builds upon the encoder-decoder framework widely used in co-saliency detection methods and incorporates correlation-assisted spatial attention to explore intra-image regional correlations. This architecture enables CMSeg-Net to detect copy-move objects in a multi-resolution fashion, ensuring that even small and previously unseen forgery objects in complex scenes are accurately identified. Comprehensive experiments on various datasets, including CASIA-CMFD, CoMoFoD, CMF, and FakeParaEgg, demonstrate CMSeg-Net’s effectiveness and its generalizability against out-of-domain data with unseen attacks.

REFERENCES

- [1] A. McCook, "Cancer researcher at the ohio state university resigns following multiple misconduct findings," *Retraction Watch*, 2018. [Online]. Available: <https://www.science.org/content/article/cancer-researcher-ohio-state-university-resigns-following-multiple-misconduct-findings>
- [2] C. Piller, "Blots on a field?" *Science (New York, NY)*, vol. 377, no. 6604, pp. 358–363, 2022.
- [3] J. Kaiser, "'i should have done better.'stanford head steps down," *Science (New York, NY)*, vol. 381, no. 6656, pp. 366–367, 2023.
- [4] H. Thorp, "Genuine images in 2024," pp. 7–7, 2024.
- [5] H.-C. Shao, "Unveiling vestiges of man-made modifications on molecular-biological experiment images," in *Proc. IEEE Glob. Conf. Signal Inf. Process.*, 2018, pp. 534–538.
- [6] E. Bik, A. Casadevall, and F. Fang, "The prevalence of inappropriate image duplication in biomedical research publications," *mBio*, vol. 7, no. 3, pp. 10–1128, 2016.
- [7] "ICIP 2022 Challenge: parasitic egg detection and classification in microscopic images," <https://icip2022challenge.piclabs.ai/>, accessed: 2023-09-07.
- [8] N. Anantrasirichai, T. Chalidabhongse, D. Palasuwan, K. Narue-natthanaset, T. Kobchaisawat, N. Nunthanasup, K. Boonpeng, X. Ma, and A. Achim, "Icip 2022 challenge on parasitic egg detection and classification in microscopic images: Dataset, methods and results," in *Proc. IEEE Int. Conf. Image Process.*, 2022, pp. 4306–4310.
- [9] J.-L. Zhong and C.-M. Pun, "An end-to-end dense-inceptionnet for image copy-move forgery detection," *IEEE Trans. Inf. Forensics Secur.*, vol. 15, pp. 2134–2146, 2020.
- [10] P. Zhou, X. Han, V. Morariu, and L. Davis, "Learning rich features for image manipulation detection," in *Proc. IEEE/CVF Conf. Comput. Vis. Pattern Recog.*, 2018, pp. 1053–1061.
- [11] Y. Wu, W. Abd-Almageed, and P. Natarajan, "Busternet: Detecting copy-move image forgery with source/target localization," in *Proc. European Con. Comput. Vis.*, 2018, pp. 168–184.
- [12] Y. Wu, W. AbdAlmageed, and P. Natarajan, "Mantra-net: Manipulation tracing network for detection and localization of image forgeries with anomalous features," in *Proc. IEEE/CVF Conf. Comput. Vis. Pattern Recog.*, 2019, pp. 9543–9552.
- [13] X. Bi, Y. Wei, B. Xiao, and W. Li, "Rru-net: The ringed residual u-net for image splicing forgery detection," in *Proc. IEEE/CVF Conf. Comput. Vis. Pattern Recog. Workshops*, 2019, pp. 1–10.
- [14] A. Islam, C. Long, A. Basharat, and A. Hoogs, "Doa-gan: Dual-order attentive generative adversarial network for image copy-move forgery detection and localization," in *Proc. IEEE/CVF Conf. Comput. Vis. Pattern Recog.*, 2020, pp. 4676–4685.
- [15] Y. Liu, C. Xia, X. Zhu, and S. Xu, "Two-stage copy-move forgery detection with self deep matching and proposal superglue," *IEEE Trans. Image Process.*, vol. 31, pp. 541–555, 2022.
- [16] Y. Liu, C. Xia, S. Xiao, Q. Guan, W. Dong, Y. Zhang, and N. Yu, "Cmfddformer: Transformer-based copy-move forgery detection with continual learning," *arXiv preprint arXiv:2311.13263*, 2023.
- [17] S. Weng, T. Zhu, T. Zhang, and C. Zhang, "Ucm-net: A u-net-like tampered-region-related framework for copy-move forgery detection," *IEEE Trans. Multimedia*, pp. 750–763, 2024.
- [18] S. Zhang, W. Ren, X. Tan, Z.-J. Wang, Y. Liu, J. Zhang, X. Zhang, and X. Cao, "Semantic-aware dehazing network with adaptive feature fusion," *IEEE Trans. Cybern.*, vol. 53, no. 1, pp. 454–467, 2021.
- [19] S. Zhang, X. Zhang, S. Wan, W. Ren, L. Zhao, and L. Shen, "Generative adversarial and self-supervised dehazing network," *IEEE Trans. Ind. Inform.*, vol. 20, no. 3, pp. 4187–4197, 2024.
- [20] D. Cozzolino, G. Poggi, and L. Verdoliva, "Efficient dense-field copy-move forgery detection," *IEEE Trans. Inf. Forensics Secur.*, vol. 10, no. 11, pp. 2284–2297, 2015.
- [21] C.-M. Pun, X.-C. Yuan, and X.-L. Bi, "Image forgery detection using adaptive oversegmentation and feature point matching," *IEEE Trans. Inf. Forensics Secur.*, vol. 10, no. 8, pp. 1705–1716, 2015.
- [22] Y. Li and J. Zhou, "Fast and effective image copy-move forgery detection via hierarchical feature point matching," *IEEE Trans. Inf. Forensics Secur.*, vol. 14, no. 5, pp. 1307–1322, 2019.
- [23] Z. Zhang, W. Jin, J. Xu, and M.-M. Cheng, "Gradient-induced co-saliency detection," in *Proc. European Con. Comput. Vis.*, 2020, pp. 455–472.
- [24] K. Zhang, M. Dong, B. Liu, X.-T. Yuan, and Q. Liu, "Deepcag: Co-saliency detection via semantic-aware contrast gromov-wasserstein distance," in *Proc. IEEE/CVF Conf. Comput. Vis. Pattern Recog.*, 2021, pp. 13 703–13 712.
- [25] M. Sandler, A. Howard, M. Zhu, A. Zhmoginov, and L.-C. Chen, "Mobilenetv2: Inverted residuals and linear bottlenecks," in *Proc. IEEE/CVF Conf. Comput. Vis. Pattern Recog.*, 2018, pp. 4510–4520.
- [26] S. Woo, J. Park, J.-Y. Lee, and I. Kweon, "Cbam: Convolutional block attention module," in *Proc. European Con. Comput. Vis.*, 2018, pp. 3–19.
- [27] H. Fu, J. Chen, G. Papandreou, I. Kokkinos, K. Murphy, and A. Yuille, "Deeplab: Semantic image segmentation with deep convolutional nets, atrous convolution, and fully connected crfs," *IEEE Trans. Pattern Anal. Mach. Intell.*, vol. 40, no. 4, pp. 834–848, 2017.
- [28] J. Deng, W. Dong, R. Socher, L.-J. Li, K. Li, and L. Fei-Fei, "Imagenet: A large-scale hierarchical image database," in *Proc. IEEE/CVF Conf. Comput. Vis. Pattern Recog.*, 2009, pp. 248–255.
- [29] H.-C. Shao, W.-L. Hwang, and Y.-C. Chen, "Optimal multiresolution blending of confocal microscope images," *IEEE Trans. Biomed. Eng.*, vol. 59, no. 2, pp. 531–541, 2011.
- [30] H.-C. Shao, S.-C. Wu, Y.-L. Chuo, J.-H. Lin, Y.-R. Liao, and T.-Y. Tseng, "Rgbt2hs-net: Reconstructing a hyper-spectral volume from an rgb-t stack via an attention-powered multiresolution framework," in *Proc. IEEE Int. Conf. Acoust. Speech Signal Process. Workshops*, 2024, pp. 83–84.
- [31] D. Tralic, I. Zupancic, S. Grgic, and M. Grgic, "Comofod—new database for copy-move forgery detection," in *Proc. ELMAR-2013*, 2013, pp. 49–54.
- [32] N. Warif, A. Wahab, M. Idris, R. Salleh, and F. Othman, "Sift-symmetry: A robust detection method for copy-move forgery with reflection attack," *J. Vis. Commun. Image Represent.*, vol. 46, pp. 219–232, 2017.
- [33] "Rembg," <https://github.com/danielgatis/rembg>, accessed: 2023-09-10.
- [34] J. Dong, W. Wang, and T. Tan, "Casia image tampering detection evaluation database," in *Proc. IEEE China Summit Int. Conf. Signal Inf. Process.*, 2013, pp. 422–426.
- [35] O. Ronneberger, P. Fischer, and T. Brox, "U-net: Convolutional networks for biomedical image segmentation," in *Proc. Med. Image Comput. Comput.-Assist. Interv.*, 2015, pp. 234–241.
- [36] Y. Zhu, C. Chen, G. Yan, Y. Guo, and Y. Dong, "Ar-net: Adaptive attention and residual refinement network for copy-move forgery detection," *IEEE Trans. Ind. Inform.*, vol. 16, no. 10, pp. 6714–6723, 2020.
- [37] Q. Li, C. Wang, X. Zhou, and Z. Qin, "Image copy-move forgery detection and localization based on super-bpd segmentation and dcnn," *Sci. Rep.*, vol. 12, no. 1, p. 14987, 2022.